# Distinct sets of tethering complexes, SNARE complexes, and Rab GTPases mediate membrane fusion at the vacuole in Arabidopsis

Kodai Takemoto[a,b], Kazuo Ebine[a,c], Jana Christin Askani[d], Falco Krüger[d], Zaida Andrés Gonzalez[d], Emi Ito[e], Tatsuaki Goh[f], Karin Schumacher[d], Akihiko Nakano[b,g], and Takashi Ueda[a,c,1]

[a]Division of Cellular Dynamics, National Institute for Basic Biology, 444-8585 Okazaki, Aichi, Japan; [b]Department of Biological Sciences, Graduate School of Science, The University of Tokyo, 113-0033 Tokyo, Japan; [c]Department of Basic Biology, SOKENDAI (Graduate University for Advanced Studies), 444-8585 Okazaki, Aichi, Japan; [d]Department of Plant Developmental Biology, Centre for Organismal Studies, Heidelberg University, 69120 Heidelberg, Germany; [e]Department of Natural Sciences, International Christian University, 181-8585 Tokyo, Japan; [f]Graduate School of Biological Sciences, Nara Institute of Science and Technology, Ikoma, 630-0192 Nara, Japan; and [g]Live Cell Super-Resolution Imaging Research Team, RIKEN Center for Advanced Photonics, Wako, 351-0198 Saitama, Japan

Edited by Natasha V. Raikhel, Center for Plant Cell Biology, Riverside, CA, and approved January 26, 2018 (received for review October 13, 2017)

**Membrane trafficking plays pivotal roles in various cellular activities and higher-order functions of eukaryotes and requires tethering factors to mediate contact between transport intermediates and target membranes. Two evolutionarily conserved tethering complexes, homotypic fusion and protein sorting (HOPS) and class C core vacuole/endosome tethering (CORVET), are known to act in endosomal/vacuolar transport in yeast and animals. Both complexes share a core subcomplex consisting of Vps11, Vps18, Vps16, and Vps33, and in addition to this core, HOPS contains Vps39 and Vps41, whereas CORVET contains Vps3 and Vps8. HOPS and CORVET subunits are also conserved in the model plant Arabidopsis. However, vacuolar trafficking in plants occurs through multiple unique transport pathways, and how these conserved tethering complexes mediate endosomal/vacuolar transport in plants has remained elusive. In this study, we investigated the functions of VPS18, VPS3, and VPS39, which are core complex, CORVET-specific, and HOPS-specific subunits, respectively. Impairment of these tethering proteins resulted in embryonic lethality, distinctly altering vacuolar morphology and perturbing transport of a vacuolar membrane protein. CORVET interacted with canonical RAB5 and a plant-specific R-soluble NSF attachment protein receptor (SNARE), VAMP727, which mediates fusion between endosomes and the vacuole, whereas HOPS interacted with RAB7 and another R-SNARE, VAMP713, which likely mediates homotypic vacuolar fusion. These results indicate that CORVET and HOPS act in distinct vacuolar trafficking pathways in plant cells, unlike those of nonplant systems that involve sequential action of these tethering complexes during vacuolar/lysosomal trafficking. These results highlight a unique diversification of vacuolar/lysosomal transport that arose during plant evolution, using evolutionarily conserved tethering components.**

HOPS | CORVET | RAB GTPase | SNARE | vacuolar transport

Plant vacuoles have diverse and specialized functions, including storage of numerous materials, recycling and degradation of cellular components, osmoregulation, coloring flowers and fruits, and filling space for cell elongation (1). In association with these complex functions, plants have evolved unique vacuolar trafficking mechanisms. For example, newly synthesized vacuolar proteins are transported to the vacuole via multiple transport pathways, which are regulated by mechanisms distinct from animal and yeast lysosomal/vacuolar trafficking pathways (2). The majority of de novo-synthesized vacuolar proteins are transported through the *trans*-Golgi network (TGN). In plants, the TGN is also known to act as the early endosome in the endocytic pathway (3), which further highlights the unique organization of endocytic/vacuolar transport in plant cells.

Despite the unique diversification of the plant vacuolar/endocytic transport system, the majority of transport components are shared between plants and nonplant systems. Rab GTPase is a key regulator for targeting and docking of transport intermediates, such as membrane vesicles, to target membranes, and promoting assembly of tethering complexes that mediate attachment of specific transport vesicles/organelles to their destination membranes. RAB5 and RAB7 are evolutionarily conserved subgroups of Rab GTPase, which in animal systems act in early and late endosomal trafficking, respectively. Although these subgroups are conserved in plants and act in endosomal/vacuolar trafficking, their functions seem to have diverged from those of their orthologs in animals. For example, plant RAB5 mainly resides on multivesiculated late endosomes, rather than on early endosomes (4). Some vacuolar membrane proteins are transported through a RAB5-dependent, RAB7-independent pathway (2), whereas a similar transport pathway has not been identified in mammals. Conversely, in mammalian cells, RAB5 mediates homotypic fusion between early endosomes, although homotypic early endosomal/TGN fusion has not been described in plant cells. In addition to canonical RAB5, plants are also equipped with a plant-specific RAB5 variant, the ARA6 group, which is another peculiarity specific to plant endosomal transport (5). Unlike canonical RAB5, which is isoprenylated

## Significance

Plant vacuoles play unique roles such as storage and coloring, in addition to lysosomal/vacuolar functions shared by eukaryotes: degradation and recycling of waste. To fulfill these complex and specialized functions, plant vacuolar trafficking occurs through multiple, uniquely regulated transport pathways. Two evolutionarily conserved tethering complexes, homotypic fusion and protein sorting (HOPS) and class C core vacuole/endosome tethering (CORVET), are involved in lysosomal/vacuolar trafficking in nonplant systems, although they also exist in plants. However, it remains almost entirely unknown how these tethering complexes regulate the unique aspects of plant vacuolar transport. Here, we show that HOPS and CORVET mediate distinct vacuolar trafficking pathways in coordination with different sets of soluble *N*-ethylmaleimide–sensitive factor attachment protein receptor (SNARE) proteins and RAB GTPase. Our findings provide further evidence for the unique evolutionary diversification of the vacuolar transport system in plants.

Author contributions: T.U. designed research; K.T., J.C.A., F.K., Z.A.G., and K.S. performed research; K.E., E.I., and T.G. contributed new reagents/analytic tools; F.K. analyzed data; K.T. and T.U. wrote the paper; and A.N. and T.U. supervised the study.

The authors declare no conflict of interest.

This article is a PNAS Direct Submission.



[1]To whom correspondence should be addressed. Email: tueda@nibb.ac.jp.

This article contains supporting information online at www.pnas.org/lookup/suppl/doi:10.1073/pnas.1717839115/-/DCSupplemental.

Published online February 20, 2018.

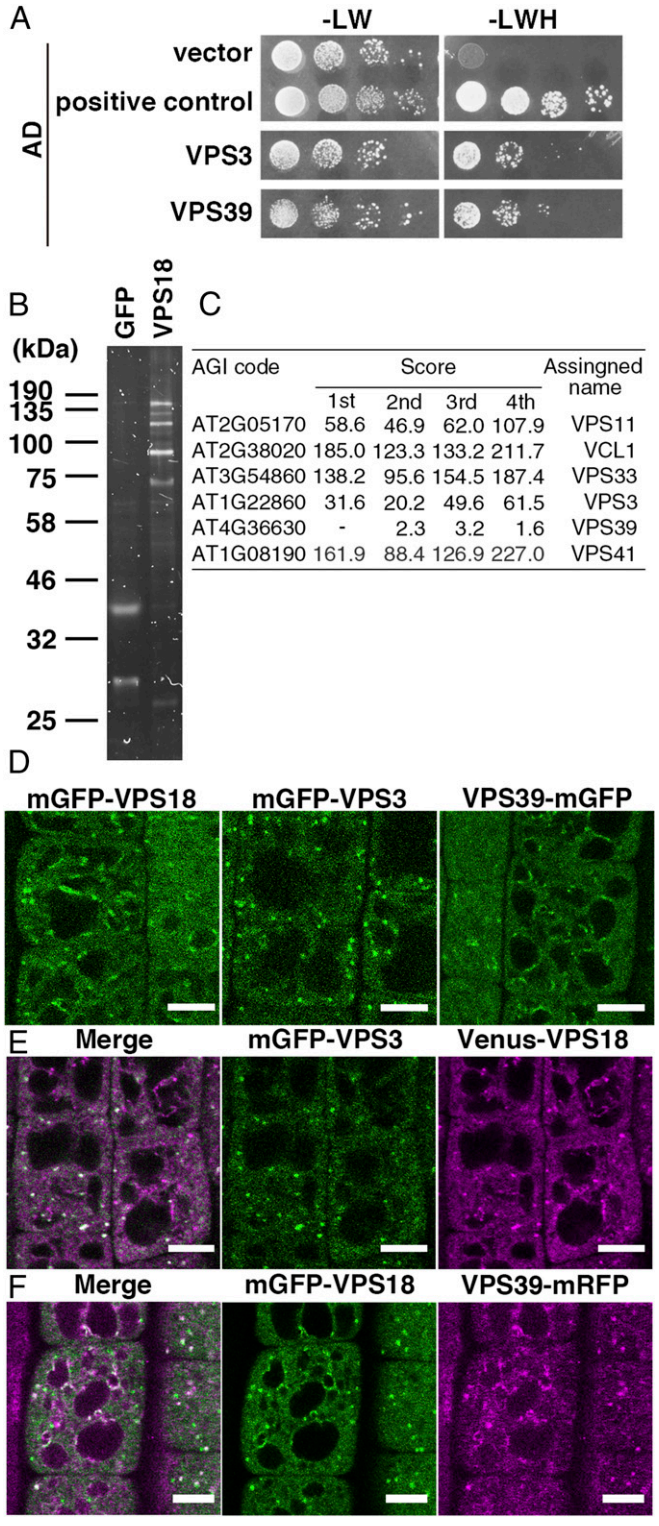


| AGI code | Score | | | | Assingned name |
|---|---|---|---|---|---|
| | 1st | 2nd | 3rd | 4th | |
| AT2G05170 | 58.6 | 46.9 | 62.0 | 107.9 | VPS11 |
| AT2G38020 | 185.0 | 123.3 | 133.2 | 211.7 | VCL1 |
| AT3G54860 | 138.2 | 95.6 | 154.5 | 187.4 | VPS33 |
| AT1G22860 | 31.6 | 20.2 | 49.6 | 61.5 | VPS3 |
| AT4G36630 | - | 2.3 | 3.2 | 1.6 | VPS39 |
| AT1G08190 | 161.9 | 88.4 | 126.9 | 227.0 | VPS41 |

**Fig. 1.** CORVET and HOPS complexes in Arabidopsis. (*A*) Interactions between VPS11 and VPS3 or VPS39 were tested by yeast two-hybrid assays. VPS11 was expressed as a fusion protein with the DNA BD, and VPS3 and VPS39 were expressed as fusions with a transcriptional AD. Interaction between BD-VPS9a and AD-ARA7$^{S24N}$ is shown as positive control. Interactions between two proteins were tested using the *HIS3* reporter gene. (*B*) Flamingo-stained SDS/PAGE gel. Proteins coprecipitated with GFP or mGFP-VPS18 (VPS18) from plant lysates were loaded. (*C*) Summary of CORVET and HOPS subunits coprecipitated with VPS18 identified by mass spectrometry in four independent experiments. Values in the score column represent XCorr scores, which represent the sum of the ion scores of all peptide sequences matching with the database. (*D*) Subcellular localization of mGFP-tagged VPS18, VPS3, and VPS39 in root epidermal cells of 5-d-old seedlings. (*E* and *F*) Colocalization analysis of Venus-VPS18 and mGFP-VPS3 (*E*) and mGFP-VPS18 and VPS39-mRFP (*F*) in root epidermal cells of 5-d-old seedlings. (Scale bars, 5 μm.)

at the C terminus, ARA6 is fatty-acylated at the N terminus, and it seemingly acts in a counteracting fashion to RAB5 (6). The genome of Arabidopsis harbors three RAB5 members: two canonical RAB5 genes, *ARA7*/*RABF2b* and *RHA1*/*RABF2a*, and plant-specific *ARA6*/*RABF1* (6, 7).

Soluble NSF attachment protein receptor (SNARE) is another key component of the membrane trafficking machinery. SNARE proteins are divided into two categories, R- and Q-SNAREs, depending on the amino acid at the 0-layer in the helical SNARE domain. Q-SNAREs are further divided into Qa-, Qb-, Qc, and Qb+c-SNAREs according to sequence similarity (8). One R-SNARE and three Q-SNAREs, one from each of the Q-SNARE subgroups (or two Q-SNAREs in the case of Qa- with Qb+c-SNARE), assemble into a tight complex, leading to fusion between R-SNARE-bearing and Q-SNARE-containing membranes (8). Two distinct vacuolar SNARE complexes have been identified in Arabidopsis: one complex consists of Qa-SYP22, Qb-VTI11, Qc-SYP5, and R-VAMP71, and the other contains R-VAMP727 instead of VAMP71 (5, 9). VAMP727, which is unique to the plant lineage, harbors a characteristic insertion in its N-terminal longin domain. VAMP727 has been shown to mediate membrane fusion between multivesicular endosomes and the vacuole (10), although whether the two vacuolar SNARE complexes are functionally different and how they are regulated during vacuolar transport remain unknown.

Endosomal/vacuolar RAB GTPases and SNARE complexes are functionally connected by tethering complexes, which interact with both RAB GTPases and SNARE proteins to mediate tethering of two membranes before membrane fusion (8). In yeast, two hexameric tethering complexes, homotypic fusion and protein sorting (HOPS) and class C core vacuole/endosome tethering (CORVET), have been shown to mediate transport from the endosome to the vacuole (11, 12). Both complexes share a core subcomplex composed of Vps11, Vps18, Vps16, and Vps33 (13), and in addition, HOPS contains Vps39 and Vps41 (12), whereas CORVET contains Vps3 and Vps8 (11). HOPS interacts with RAB7-like Ypt7 and vacuolar SNARE proteins including Vam3, a homolog of plant SYP22 (12), to mediate membrane fusion between late endosomes and vacuole and controls homotypic fusion of vacuolar membranes (14–16). Conversely, CORVET binds to RAB5-like Vps21 and mediates tethering of Vps21-positive endosomes (17). The functions of HOPS and CORVET complexes are largely conserved in mammalian cells as well (18–22).

In plants, homologs for all subunits of the HOPS and CORVET complexes are conserved (23, 24), some of which play essential roles in embryogenesis and/or gametophyte functions. The Arabidopsis *vacuoless1* (*vcl1*) mutant, which harbors a mutation in the *VPS16* gene, exhibits severe defects in vacuole biogenesis (25). Recently, *VPS11* and *VPS41* were also reported to be required for vacuole biogenesis during embryogenesis and pollen tube growth (26, 27). In contrast, functions of CORVET-specific subunits in endosomal/vacuolar trafficking have not yet been explored in plants, and the functional linkages between RAB GTPases, tethering complexes, and SNARE complexes involved in endosomal/vacuolar transport remain totally unknown. To elucidate how these evolutionarily conserved components fulfill their functions in the uniquely developed plant endosomal/vacuolar transport system, we conducted comparative analyses of VPS18, VPS3, and VPS39, which represent core complex, CORVET-specific, and HOPS-specific subunits, respectively.

We found that CORVET and HOPS specifically interact with RAB5 and RAB7, respectively, and act in separate vacuolar trafficking pathways involving distinct sets of SNARE proteins. Our results provide further evidence that plants have evolved unique endosomal/vacuolar trafficking pathways, which has been achieved by coordinating evolutionarily conserved components with unique plant-specific machinery.

## Results

**HOPS and CORVET Complexes in Arabidopsis.** The Arabidopsis genome contains homologs of all subunits for the HOPS and CORVET complexes (23, 24). Although formation of the core complex by VPS11, VCL1/VPS16, and VPS33 has been reported (28), it is still unclear whether subunits specific to HOPS and CORVET also assemble into their respective complexes in plants. To examine protein–protein interactions of HOPS- and CORVET-specific subunits with the core complex, we performed yeast two-hybrid assays using DNA binding domain (BD)-fused VPS11 and activation domain (AD)-fused VPS3 or VPS39. As shown in Fig. 1*A*, VPS11 interacted with both VPS3 and VPS39 in yeast (Fig. 1*A*). We then investigated whether HOPS and CORVET complexes form in planta. Monomeric green fluorescent protein (mGFP)-tagged VPS18 was expressed in Arabidopsis and immunoprecipitated using an anti-GFP antibody, and interacting proteins were analyzed by mass spectrometry. We detected all subunits of HOPS and CORVET except for VPS8 in the precipitate, whereas free GFP did not precipitate any subunits of these complexes (Fig. 1 *B* and *C* and Dataset S1). These results indicate that HOPS and CORVET complexes exist in Arabidopsis cells.

**Subcellular Localization of HOPS and CORVET Subunits.** To examine the subcellular localization of HOPS and CORVET, we expressed mGFP-VPS18, mGFP-VPS3, and VPS39-mGFP in *vps18*, *vps3*, and *vps39* mutants, respectively, under control of their endogenous promoters. These chimeric proteins rescued the lethal phenotypes of the corresponding mutants (described here), demonstrating the functionality of the chimeric proteins (*SI Appendix*, Fig. S1). Confocal microscopy revealed that mGFP-VPS18 localized to subdomains of the vacuolar membrane and punctate compartments in the cytoplasm, with faintly dispersed distribution in the cytosol. mGFP-VPS3 was primarily targeted to cytoplasmic punctate structures with no detectable vacuolar membrane localization, whereas VPS39-mGFP was mainly observed on subdomains of the vacuolar membrane with a small number of punctate structures in the cytoplasm (Fig. 1*D*). We then coexpressed VPS18 with either VPS3 or VPS39 tagged with distinct fluorescent proteins, which revealed that VPS3 colocalized with VPS18 on cytoplasmic puncta, whereas VPS39 mainly colocalized with VPS18 on subdomains of the vacuolar membrane (Fig. 1 *E* and *F* and *SI Appendix*, Fig. S2). Staining with FM4-64 also indicated that mGFP-VPS18 and VPS39-mGFP were sometimes observed at the vertex zone, the

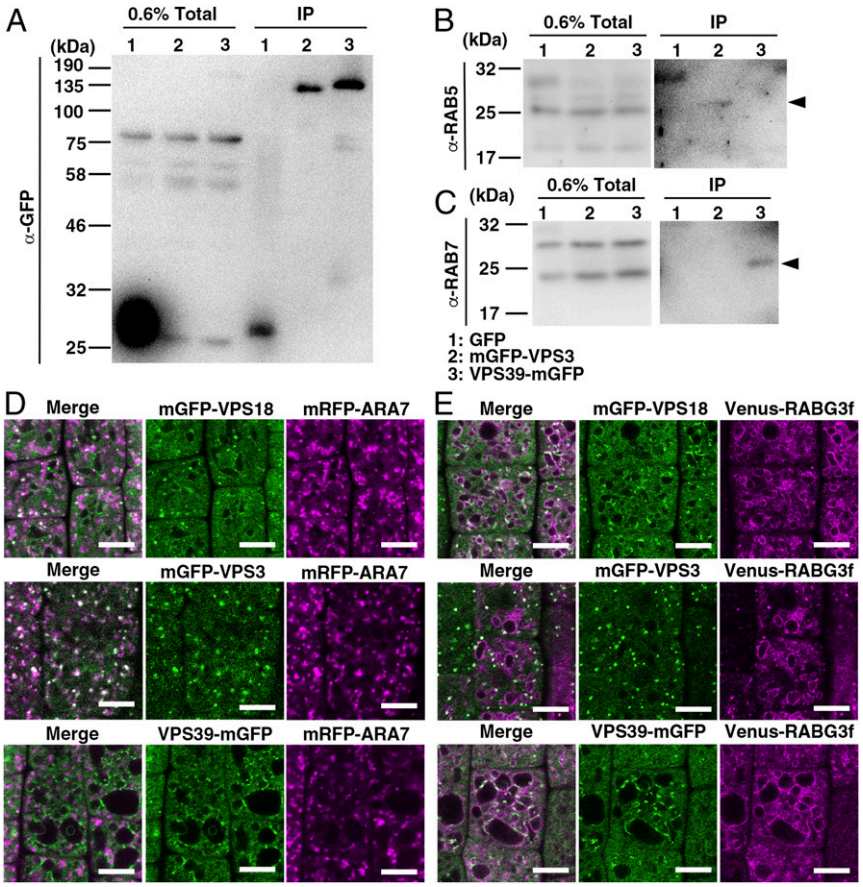


**Fig. 2.** Interaction of HOPS and CORVET with endosomal/vacuolar RAB GTPases. (*A*–*C*) Coimmunoprecipitation analysis for interaction between tethering complexes and RAB GTPases. Plant lysates prepared from transgenic plants expressing GFP, mGFP-VPS3, or VPS39-mGFP were subjected to immunoprecipitation using the anti-GFP antibody. Precipitates were used for Western blotting using anti-GFP (*A*), anti-RAB5 (*B*), and anti-RAB7 (*C*) antibodies. Arrowheads indicate RAB5 in *B* and RAB7 in *C*. (*D* and *E*) Colocalization between tethering complexes and RAB GTPases. Root epidermal cells of 5-d-old seedlings coexpressing mRFP-ARA7 and mGFP-VPS18, mGFP-VPS3, or VPS39-mGFP (*D*) and 5-d-old seedlings coexpressing Venus-RABG3f and mGFP-VPS18, mGFP-VPS3, or VPS39-mGFP (*E*) were observed. (Scale bars, 5 μm.)

ring-shaped edge of vacuole–vacuole contact sites (*SI Appendix*, Fig. S3).

**HOPS and CORVET Interact with Distinct RAB GTPases.** In yeast, CORVET and HOPS are known to interact with Vps21/RAB5 and Ypt7/RAB7, respectively, acting as effectors. We examined whether this holds true in Arabidopsis by performing coimmunoprecipitation with the lysate prepared from transgenic plants expressing mGFP-VPS3 or VPS39-mGFP. When using an anti-GFP antibody, mGFP-VPS3 coprecipitated with canonical RAB5 (ARA7 and RHA1), but not with RAB7, whereas VPS39 coprecipitated with RAB7, but not with RAB5 (Fig. 2 *A*–*C*). Thus, specific interactions between endosomal/vacuolar tethers and the Rab GTPases are conserved in plants.

To further verify these interactions, we compared the subcellular localization of HOPS and CORVET with ARA7 and a RAB7 member, RABG3f, which primarily localize to multivesicular endosomes and the vacuolar membrane, respectively (2, 5). mRFP-ARA7 exhibited strong colocalization with mGFP-VPS3 in cytoplasmic puncta, but not with VPS39-mGFP (Fig. 2*D* and *SI Appendix*, Fig. S2). Conversely, Venus-RABG3f exhibited only partial colocalization with mGFP-VPS3 at cytoplasmic punctate structures, although colocalization at subdomains of the vacuolar membrane was observed with VPS39-mGFP (Fig. 2*E* and *SI Appendix*, Figs. S2 and S4). Consistent with the hypothesis that VPS18 is a subunit of the core complex shared between HOPS and CORVET, mGFP-VPS18 exhibited colocalization with mRFP-ARA7 and Venus-RABG3f (Fig. 2 *D* and *E* and *SI Appendix*, Figs. S2 and S4). We also noticed that VPS39 and RABG3f frequently colocalized at contact sites between two vacuoles. These results strongly suggest that CORVET acts with canonical RAB5 on multivesiculated endosomes, whereas HOPS and RAB7 coordinate the tethering between homotypic vacuolar membranes.

To further investigate the relationship between tethering complexes and Rab GTPases, we next examined the effects of compromised Rab activation on the subcellular localization of HOPS and CORVET subunits. For this purpose, we expressed mGFP-tagged VPS18, VPS3, and VPS39 in the *vps9a-2* and *ccz1a ccz1b* (hereafter indicated as *ccz1ab*) backgrounds, which are mutants of nucleotide exchange factors for RAB5 and RAB7, respectively (2, 29). In *vps9a-2*, mGFP-VPS3 was dispersed through the cytosol with residual localization to punctate cytoplasmic structures, suggesting that RAB5 activation is required for efficient localization of VPS3 to multivesicular endosomes. Intriguingly, mGFP-VPS18 and VPS39-mGFP were still localized to the vacuolar membrane in *vps9a-2*, although their distribution was more uniform than in wild-type plants (Fig. 3*A*). Conversely, in *ccz1ab*, membrane attachment of VPS39-mGFP was hardly detected, whereas mGFP-VPS3 was still localized to punctate structures, some of which were dilated similarly to RAB5-positive endosomes observed in *ccz1ab* (Fig. 3*B*) (2). Localization of mGFP-VPS18 to the vacuolar membrane was also barely detected, although its endosomal localization, which was partially expanded, was retained in this mutant. Taken together, CORVET requires RAB5 activation for endosomal localization, whereas localization of HOPS on the vacuolar membrane depends on RAB7 activation.

**HOPS and CORVET Are Required for Normal Development of Arabidopsis.** We then investigated the significance of HOPS and CORVET in plant development. We examined phenotypes of *vps18*, *vps3*, and *vps39* T-DNA insertion mutants, illustrated in *SI Appendix*, Fig. S5. PCR-based genotyping of the progeny from self-pollinated heterozygous mutant plants revealed that homozygous mutants were inviable for all of three genes, and the segregation ratios of the wild-type to heterozygous mutant plants were between 1:1 and 1:2 ($VPS18^{+/+}$:$VPS18^{+/-}$ = 96:140, $VPS3^{+/+}$:$VPS3^{+/-}$ = 105:144, and $VPS39^{+/+}$:$VPS39^{+/-}$ = 59:105), suggesting that the homozygous mutations resulted in embryonic lethality. Consistently for all three genes, yellowish seeds were observed in siliques of heterozygous plants (Fig. 4*A*), in which developmentally retarded or abnormally shaped embryos were observed (Fig. 4*B*). To investigate whether the mutations also affected gametophyte functions, we carried out a reciprocal crossing analysis. Each mutation was heritable via female gametophytes at slightly lower efficiency, but transmission of the mutations from male gametophytes was markedly affected (*SI Appendix*, Table S1). Thus, the functions of HOPS and CORVET are required for normal gametophyte function and embryogenesis in Arabidopsis.

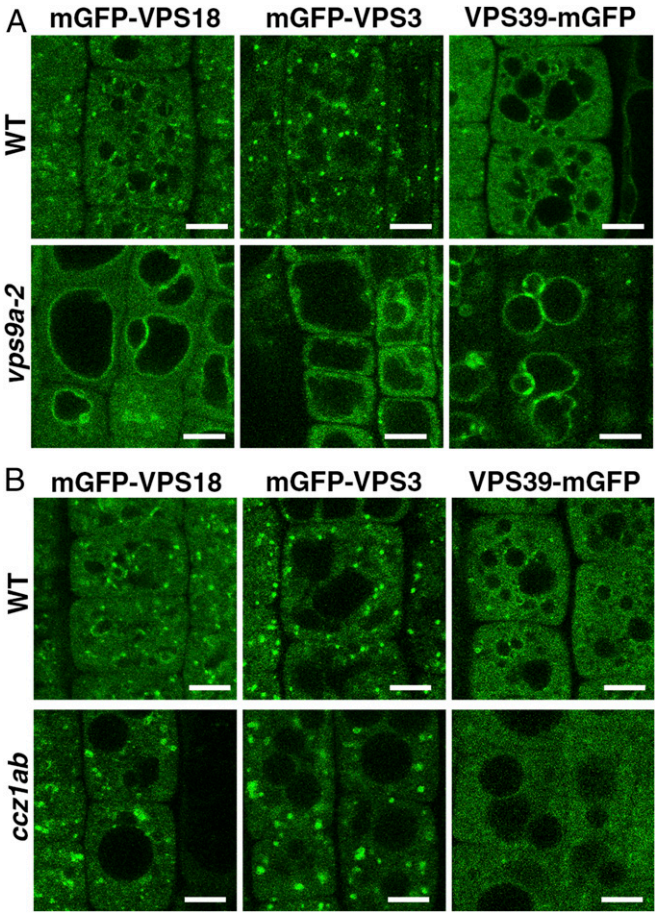


**Fig. 3.** Effects of defective activation of RAB5 and RAB7 on localization of HOPS and CORVET. mGFP-VPS18, mGFP-VPS3, and VPS39-mGFP were expressed in *vps9a-2* (defrective in RAB5 activation) (*A*) and *ccz1ab* (defective in RAB7 activation) (*B*) and observed in root epidermal cells of 5-d-old seedlings. (Scale bars, 5 μm.)

To examine whether the functions of HOPS and CORVET are also required in later developmental stages, we analyzed the effects of the conditional knockdown of *VPS3*, *VPS8*, and *VPS39*, using the dexamethasone (DEX)-inducible amiRNA system. In contrast to the DEX treatment of wild-type plants and knockdown of the HOPS-specific subunit VPS39, DEX-induced knockdown of CORVET-specific subunits VPS3 and VPS8 resulted in abnormal root morphology (Fig. 4*C*), indicating that CORVET plays an essential role in Arabidopsis root development. DEX-induced knockdown of VPS39 led to an altered vacuolar morphology showing fragmented round vacuoles in several independent transgenic lines (Fig. 4*D* and *SI Appendix*, Fig. S6*A*), confirming a critical role of HOPS in central vacuole formation in later developmental stages. Intriguingly, we did not observe fragmented,

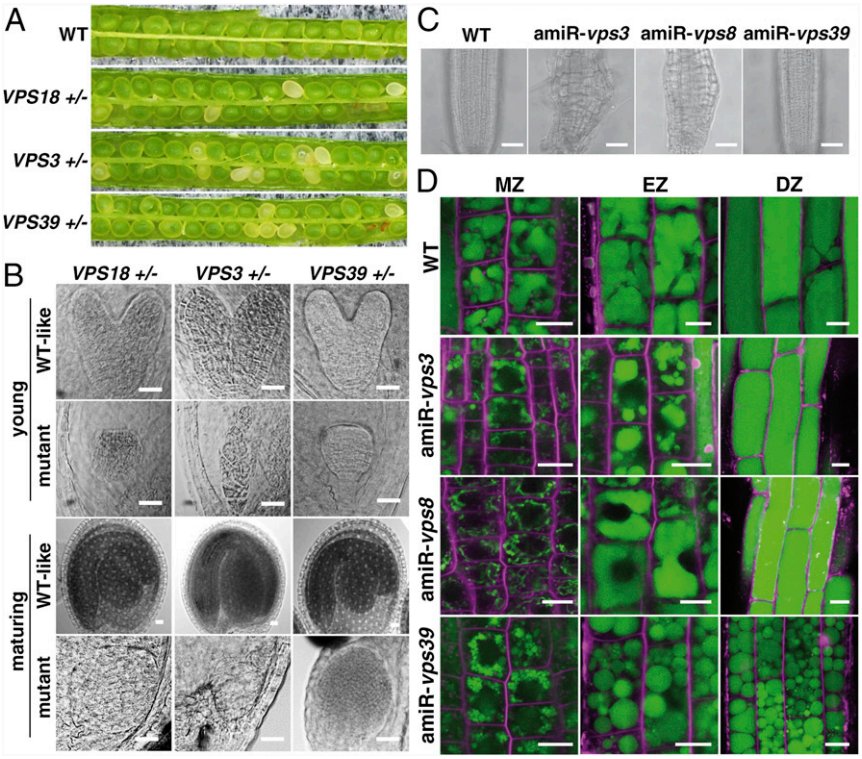


**Fig. 4.** Effects of impairment of HOPS and CORVET function. (*A*) Siliques collected from Arabidopsis plants with the indicated genotypes are shown. The mutant seeds exhibit a yellowish appearance. (*B*) Nomarski images of cleared embryos observed in young (*Upper*) and maturing (*Lower*) siliques collected from plants with the indicated genotypes. Siblings in the same siliques with wild type-like (WT-like) and aberrant appearance (mutant) are presented. (Scale bars, 20 μm.) (*C* and *D*) Effects of conditional knockdown of CORVET and HOPS subunits. Knock down of *VPS3* and *VPS8* by DEX induction of amiRNA resulted in abnormal root morphology (*C*). On *VPS39* knockdown, vacuoles, visualized by BCECF staining, were fragmented (*D*). DZ, differentiation zone; EZ, elongation zone; MZ, meristematic zone. (Scale bars, 50 μm for *C*, and 10 μm for *D*.)

but more reticulated, vacuoles in the meristematic zone when CORVET-specific subunits were knocked down (Fig. 4*D*). This result suggested that HOPS and CORVET regulate distinct trafficking events, which are differently required for vacuole biogenesis.

**Distinct Requirements for HOPS and CORVET in Vacuolar Transport.** We previously reported that vacuolar transport in Arabidopsis occurs through multiple transport pathways, with distinct functions for RAB5 and RAB7 (2). Among these pathways, SYP22 is transported through a RAB5-dependent, RAB7-independent pathway in root epidermis cells. We further investigated requirement for HOPS and CORVET in this trafficking pathway by expressing mRFP-SYP22 in *vsp18*, *vps3*, and *vps39* embryos. In WT-like embryos from siliques of heterozygous mutants, mRFP-SYP22 localized to the vacuolar membrane (Fig. 5), as observed in other tissues (30). In contrast, mRFP-SYP22 was mistargeted to the plasma membrane in homozygous mutant embryos of *vps18* and *vps3*, reminiscent of SYP22 mislocalization to the plasma membrane in root epidermal cells of the *vps9a-2* mutant (2). Intriguingly, in the *vps39* mutant embryo, mRFP-SYP22 localized to punctate structures without localization to the plasma membrane (Fig. 5). The mistargeting of SYP22 to the plasma membrane in the *vps3* mutant was not the result of an absence of the vacuole in this mutant embryo, because GFP-VAMP713, which is transported to the vacuolar membrane through a distinct trafficking pathway involving the adaptor protein complex-3 (2), localized to the vacuolar membrane when coexpressed with mRFP-SYP22 in the *vps3* mutant (*SI Appendix*, Fig. S7). These results indicate that CORVET is required for vacuolar transport of SYP22, although it is dispensable for central vacuole biogenesis. We further examined the effects on endocytic and vacuolar trafficking in the CORVET and HOPS amiRNA lines. We did not detect a marked effect on bulk endocytic transport of FM4-64 to the vacuolar membrane on knockdown of CORVET- and HOPS-specific subunits (Fig. 6 *A*–*C*), probably reflecting the existence of multiple distinctly regulated late endosomal trafficking pathways in plants. However, vacuolar targeting of pHGFP-VTI11 was severely and specifically affected in DEX-treated amiR-*vps3* root epidermal cells; pHGFP-VTI11 was mistargeted to the plasma membrane, whereas it was still transported to fragmented vacuoles in amiR-*vps39* root epidermal cells (Fig. 6 *D* and *E*). Conversely, mistargeting of YFP-VAMP711 to the plasma membrane was not induced in DEX-treated amiRNA lines (Fig. 6 *F* and *G* and *SI Appendix*, Fig. S6 *B*–*D*). Instead, the efficiency of YFP-VAMP711 transport to the vacuolar membrane was significantly reduced in DEX-treated amiR-*vps39* root epidermal cells, as indicated by the fluorescence intensity ratio of vacuolar membrane and cytoplasmic punctate signal (*SI Appendix*, Fig. S6*E*). These results further indicated that CORVET is involved in a distinct vacuolar transport pathway from HOPS-mediated vacuolar transport.

**HOPS and CORVET Act with Distinct SNARE Complexes.** As described earlier, impairments in HOPS and CORVET conferred distinct effects on vacuolar morphology and transport, which strongly suggests that these tethering complexes act in different vacuolar transport events. Given the reported interaction between the HOPS and CORVET core complex with SYP22 in Arabidopsis (28), the distinct functions of HOPS and CORVET may be the result of distinct interactions with two SYP22-containing vacuolar SNARE complexes using different R-SNAREs: one containing VAMP713 and the other with VAMP727 (5, 9). To

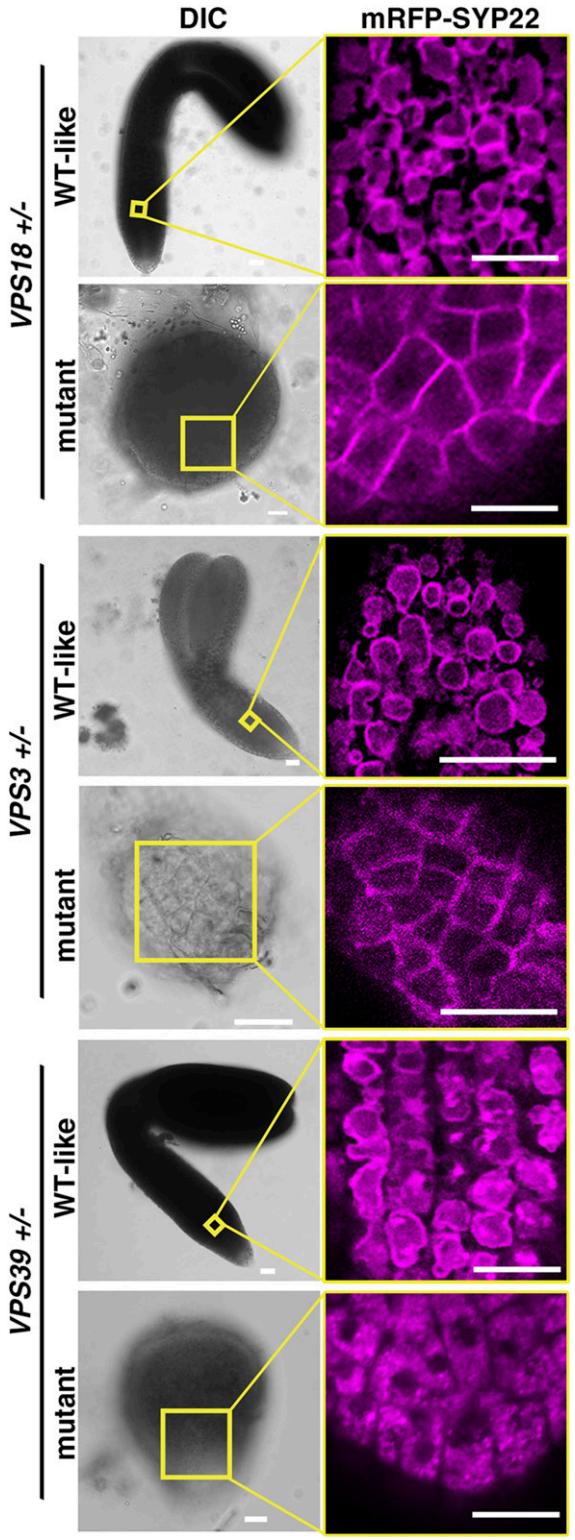


**Fig. 5.** Defective HOPS and CORVET complexes confer distinct effects on SYP22 transport. mRFP-SYP22 was expressed in plants with the indicated genotypes, and its localization was observed in developing embryos. Siblings in the same siliques with wild type-like (WT-like) and aberrant appearance (mutant) were observed. Areas in yellow squares in Nomarski images (*Left*) were observed by confocal microscopy (*Right*). (Scale bars, 20 μm.)

investigate this possibility, we compared the subcellular localization of these R-SNARE proteins with subunits specific to HOPS and CORVET. VPS39-mRFP exhibited strong colocalization with mGFP-VAMP713 at the contact sites of two vacuoles, whereas colocalization with mGFP-VAMP727 was rarely observed (Fig. 7 *A* and *B*). Conversely, mGFP-VPS3 colocalized with TagRFP-VAMP727, but not with TagRFP-VAMP713 (Fig. 7 *C* and *D*). The core complex subunit, mGFP-VPS18, partially colocalized with both R-SNARE molecules (*SI Appendix*, Figs. S2, S4, and S8). These results indicate that the two endosomal/vacuolar tethering complexes, HOPS and CORVET, mediate distinct membrane fusion events at the vacuole, which was further supported by coimmunoprecipitation analysis. When mGFP-tagged VAMP727 and VAMP713 expressed in Arabidopsis were immunoprecipitated using the anti-GFP antibody and interacting proteins were analyzed by mass spectrometry, HOPS- and CORVET-specific subunits were specifically detected in the VAMP713- and VAMP727-precipitates, respectively (Fig. 7 *E* and *F* and Dataset S2). Thus, HOPS acts with the VAMP713-containing SNARE complex to mediate membrane fusion between vacuoles, whereas CORVET promotes membrane fusion between multivesicular endosomes and the vacuole, a process mediated by the SNARE complex involving VAMP727 as its R-SNARE (10) (Fig. 8).

## Discussion

In this study, we demonstrated that CORVET and HOPS exist in plants, although they act differently from their animal and yeast counterparts in the uniquely developed plant vacuolar transport system. In budding yeast, CORVET and HOPS regulate a sequential trafficking event during endosomal maturation, which involves Rab conversion mediated by the Mon1-Ccz1 complex, an effector of Vps21 which also acts as an activating factor for Ypt7 (31). This scheme is essentially conserved in metazoan (16), suggesting a conserved regulatory mechanism of vacuolar/lysosomal transport in Opisthokonta. In plants, the vacuolar transport system has uniquely diversified during evolution to produce complex, highly specialized endosomal/vacuolar transport pathways. We previously reported that at least three distinct transport pathways operate in vacuolar transport in Arabidopsis, one of which involves both RAB5 and RAB7, whereas another requires only RAB5. The latter pathway is responsible for SYP22 transport, which corresponds to the CORVET-dependent transport pathway we identified in this study, as SYP22 also requires CORVET function for vacuolar localization. Together with the plausible involvement of the plant-specific R-SNARE VAMP727 in this pathway, which was suggested by strong colocalization and coimmunoprecipitation of CORVET and VAMP727, we propose a model of the components acting in this pathway in Fig. 8. This functional module contains RAB5, CORVET, and the VAMP727-containing SNARE complex, and is likely responsible for fusion between multivesicular endosomes and the vacuolar membrane, based on the observation that VAMP727 mediates the fusion between these membranes (10).

The other module contains RAB7, HOPS, and the VAMP71-containing SNARE complex (Fig. 8). This module likely mediates homotypic fusion between vacuoles, considering the colocalization of HOPS components and VAMP71 at the contact sites between vacuoles and the fragmented vacuole phenotype induced by depletion of VAMP71 or HOPS components (Fig. 4*D* and ref. 32). This transport pathway seems to correspond to the RAB5- and RAB7-dependent pathway described in previous work (2), given that RAB7 is activated by the SAND/MON1-CCZ1 complex, which also acts as an effector of canonical RAB5 (2, 33, 34). Consistently, impairment in RAB5 activation by the *vps9a-2* mutation resulted in altered vacuolar membrane localization of HOPS components; VPS39 and VPS18 exhibited a more uniform distribution than in wild-type plants on the vacuolar membrane. Localized RAB5 activation near the vacuolar membrane could be required for confinement of HOPS distribution, a process that may be mediated by the activating complex SAND/MON1-CCZ1 followed by confined activation of RAB7. Otherwise, unknown

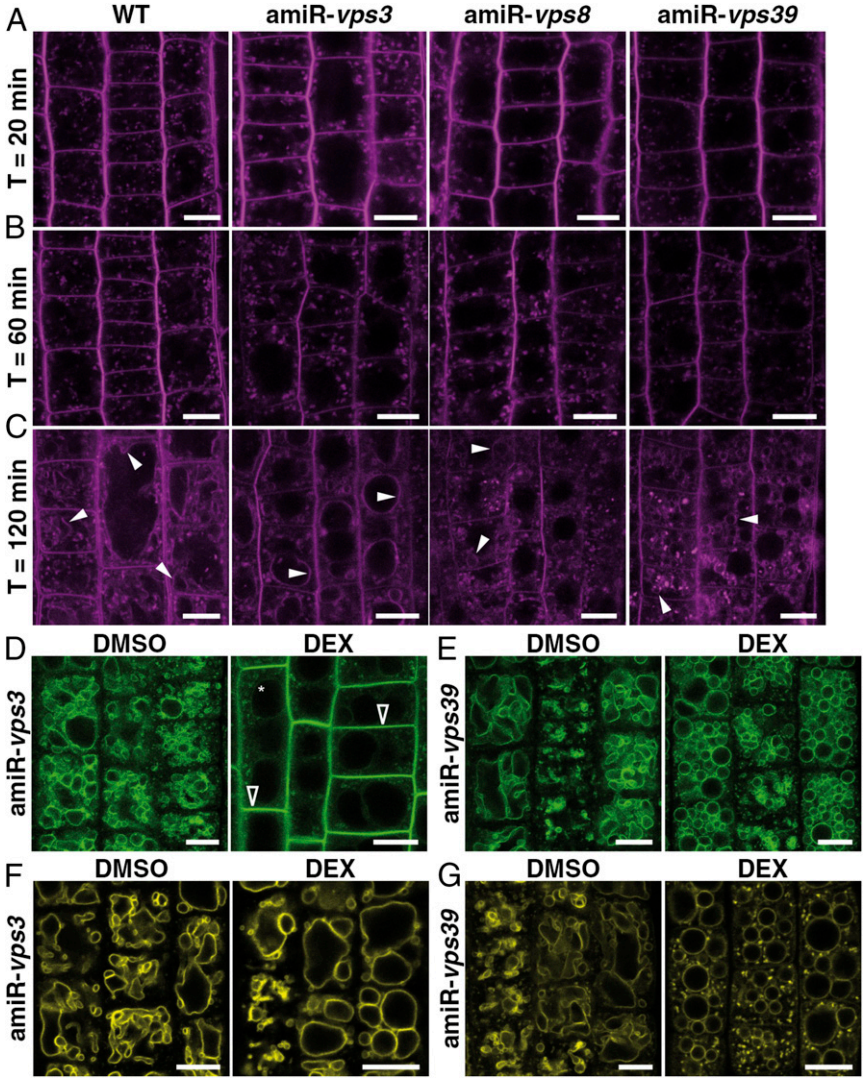


**Fig. 6.** Effects of conditional knockdown of HOPS and CORVET on endocytic and vacuolar transport. (*A*–*C*) DEX-treated WT, amiR-*vps3*, amiR-*vps8*, and amiR-*vps39* plants were stained with FM4-64 and their root epidermal cells were observed at 20 min (*A*), 60 min (*B*), and 120 min (*C*) after staining started. Closed arrowheads indicate vacuolar membrane labeling by FM4-64. (*D*–*G*) Root epidermal cells of DMSO- (*D* and *F*) or DEX-treated (*E* and *G*) amiRNA-*vps* lines coexpressing pHGFP-VTI11 (*D* and *E*) or YFP-VAMP711 (*F* and *G*) were observed. Open arrowheads indicate plasma membrane labeling. (Scale bars, 10 μm.)

components required for localization of HOPS to vacuolar membrane subdomains could be delivered to the vacuole through RAB5-dependent trafficking pathways.

Mutations in genes analyzed in this study, *vps18*, *vps3*, and *vps39*, resulted in embryonic lethality with partial defects in gametophytic functions, and similar effects have also been reported for *vps11* and *vcl1*/*vps16* (25, 26, 35). Intriguingly, the *vps41* mutation conferred a more severe effect on male gametophyte functions, resulting in male gametophytic lethality (27). It is expected that mutations in core complex components would confer stronger effects, as those mutants would be defective in both HOPS- and CORVET-dependent trafficking pathways. We also confirmed that VPS18, a subunit of the core complex, colocalized with both RAB5 and RAB7, as well as with HOPS- and CORVET-specific subunits. However, even among subunits of the core complex, the effects of loss of function varied: *vcl1*/*vps16* resulted in embryonic lethality, whereas *vps41* caused gametophytic lethality. Although the reason of this phenotypic variation is not clear at present, there may be additional gametophyte functions for some of the subunits of HOPS and CORVET, such as VPS41.

Above, we have shown that both CORVET and HOPS mediate membrane fusion at the vacuole, distinct from their sequential actions during vacuolar/lysosomal transport in animal and yeast cells. This dual-module system for vacuolar membrane fusion may have provided additional options to the plant vacuolar transport system, which has led to the evolution of a novel plant vacuolar transport pathway. This could also have been accomplished by incorporating plant-specific transport machinery components such as VAMP727.

The unique plant-specific organization of the vacuolar transport system may also be associated with plant-specific reorganization of the endocytic pathway. Homotypic early endosomal fusion, which is mediated by RAB5 and CORVET in nonplant systems, is not employed in plants. Instead, the TGN acts as the early endosome in plants (3). Recruitment of the RAB5-CORVET complex to membrane fusion events, distinct from those in nonplant systems, might have led to the plant-specific organization of the endocytic pathway. Further studies on the vacuolar and endocytic transport pathways in basal lineages of plants such as algae, chara, mosses, and liverworts would be effective for reconstituting the evolutionary

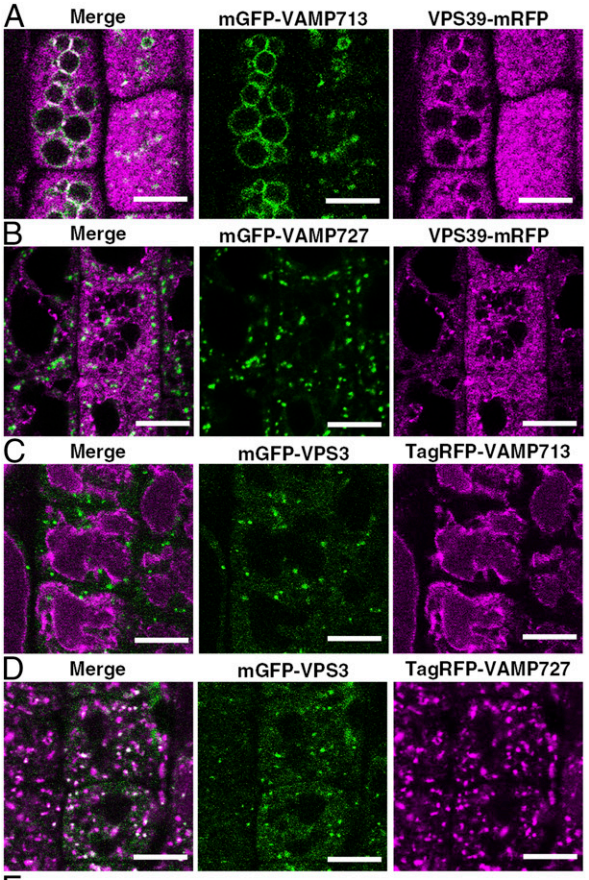


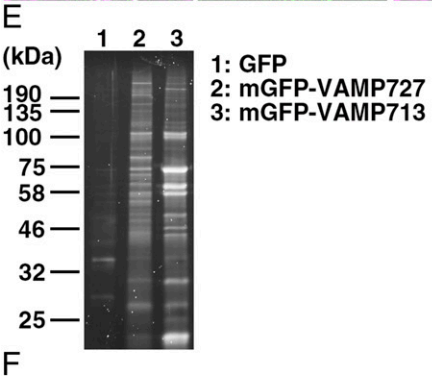


F

| AGI code | Score mGFP-VAMP727 1st | mGFP-VAMP727 2nd | mGFP-VAMP713 1st | mGFP-VAMP713 2nd | Assingned name | |
|---|---|---|---|---|---|---|
| AT2G05170 | 12.5 | 4.4 | 48.2 | 46.2 | VPS11 | Class C Core |
| AT2G38020 | 11.7 | - | 46.2 | 45.3 | VCL1 | |
| AT1G12470 | 28.6 | 16.3 | 70.9 | 65.6 | VPS18 | |
| AT3G54860 | 9.4 | 5.7 | 27.8 | 35.4 | VPS33 | |
| AT1G22860 | 11.9 | 6.4 | - | - | VPS3 | CORVET specific |
| AT4G00800 | 10.7 | 18.3 | - | - | VPS8 | |
| AT4G36630 | - | - | 49.3 | 37.2 | VPS39 | HOPS specific |
| AT1G08190 | - | - | 31.6 | 41.9 | VPS41 | |

**Fig. 7.** HOPS and CORVET colocalize and interact with distinct R-SNAREs. (*A* and *B*) VPS39-mRFP was coexpressed with mGFP-VAMP713 (*A*) or mGFP-VAMP727 (*B*). (*C* and *D*) mGFP-VPS3 was coexpressed with TagRFP-VAMP713 (*C*) or TagRFP-VAMP727 (*D*). (Scale bars, 5 μm.) (*E*) Flamingo-stained SDS/PAGE gel. Proteins coprecipitated with GFP, mGFP-VAMP727, or mGFP-VAMP713 from plant lysates were loaded. (*F*) Summary of CORVET and HOPS subunits coprecipitated with VAMP proteins identified by mass spectrometry in two independent experiments. Values in the score column represent XCorr scores. Free GFP did not precipitates any subunits of CORVET and HOPS.

path that plants followed to develop their unique vacuolar/endosomal system.

## Materials and Methods

**Plant Materials and Plasmids.** Arabidopsis *vps3* (SALK_0428653) and *vps39* (SALK_092095) mutants were obtained from the ABRC. The mutants were backcrossed at least three times to wild-type Arabidopsis (Col-0). The *vps18* mutant and transgenic plants expressing GFP were kindly provided by M. T. Morita and S. Mano, respectively (36, 37). The *vps9a-2*, *ccz1a*, and *ccz1b* mutants were obtained from our laboratory stocks (2, 29). Construction of transgenic plants expressing mRFP-ARA7, Venus-RABG3f, TagRFP-VAMP727, and mRFP-SYP22 expressed under their native promoters were described previously (5, 10, 38). For construction of mGFP-VAMP713, mGFP-VAMP727, and ARA6-mGFP, the mutation for monomerization (A206K, ref. 39) was introduced by PCR mutagenesis to reported constructs of GFP-VAMP713, GFP-VAMP727, and ARA6-GFP, respectively (5, 10, 29, 38). The transgenic line of YFP-VAMP711 (WAVE9Y) was obtained from the WAVE collection (40). pHGFP-VTI11 was amplified from cDNA and cloned with the GreenGate system (41) (*SI Appendix*, Table S2). For construction of transgenic plants expressing fluorescently tagged VPS18, VPS3, VPS39, and VAMP713, cDNA for mGFP, Venus, TagRFP, or mRFP was inserted in front of the start or stop codon of each gene. The genomic fragments contained coding regions and 2.0 and 1.0 kb of the 5′- and 3′-flanking sequences, respectively, for *VPS18* (At1g12470), 2.0 and 0.9 kb of the 5′- and 3′-flanking sequences, respectively, for *VPS3* (At1g22860), and 2.0 and 1.0 kb of the 5′- and 3′-flanking sequences, respectively, for *VPS39* (At4g36630). Chimeric genes were subcloned into pBGW or pHGW vectors (42). Transformation of Arabidopsis plants was performed by floral dipping using *Agrobacterium tumefaciens* (strain GV3101::pMP90).

To generate the knockdown of *VPS3*, *VPS8*, and *VPS39* by DEX-inducible amiRNAs, we used the WMD3 micro-RNA design tool (43) at wmd3.weigelworld.org/cgi-bin/webapp.cgi to obtain adequate amiRNA sequences and primers to mutate the endogenous miR319a precursor sequence encoded on the pRS300 plasmid following the official guidelines on this webpage (*SI Appendix*, Tables S3, S4, and S5). For subsequent cloning steps, the GreenGate system (41) was used to combine the two expression cassettes of the LhG4-GR/p6xOP DEX induction system (44, 45) on a single T-DNA. For this purpose, the primers A and B given by the WMD3 tool were modified with GreenGate compatible overhangs (*SI Appendix*, Table S5). To create the destination vectors for Arabidopsis transformation with *Agrobacterium tumefaciens* (strain ASE1 pSOUP+) the transcription factor LhG4-GR driven by the pUBQ10 promoter and the respective amiRNA under the control of the p6xOP promoter were fused with the pGGZ backbone (*SI Appendix*, Table S6 Intermediate module A, *SI Appendix*, Table S7 Intermediate module B, and *SI Appendix*, Table S8 Destination module).

**Primers.** Primers used for genotyping, cloning, and construction in this study are listed in *SI Appendix*, Table S9.

**Microscopy.** Fluorescence microscopy of root epidermal cells was performed with an LSM780 (Carl Zeiss). For single-color imaging of VPS18, VPS3, and VPS39, we observed homozygous mutant plants whose lethality was rescued by expression of their respective fluorescently tagged proteins. For colocalization

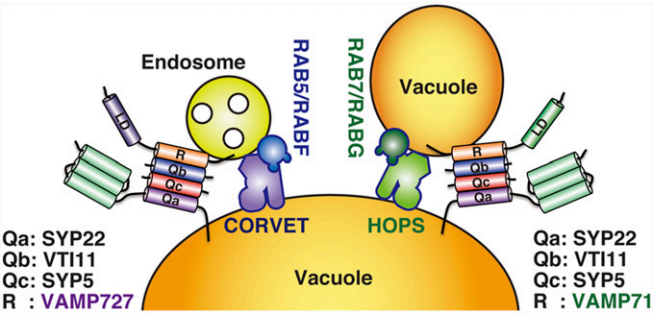


**Fig. 8.** Schematic illustration of tethering-fusion modules acting in vacuolar transport in Arabidopsis cells. Two endosomal/vacuolar tethering complexes, HOPS and CORVET, mediate distinct membrane fusion events at the vacuole; HOPS acts with the VAMP713-containing SNARE complex and RAB7 to mediate membrane fusion between vacuoles, whereas CORVET mediates membrane fusion between multivesicular endosomes and the vacuole, in coordination with RAB5 and the VAMP727-containing SNARE complex.

analysis using Venus-RABG3f, mutant plants complemented by fluorescently tagged HOPS and CORVET subunits were transformed with *Venus-RABG3f* subcloned into pBGW, and T1 plants were observed. In other multicolor localization analyses, F1 plants obtained by crossing transgenic plants were observed. For HOPS and CORVET subunits, mutant plants complemented by the fluorescently tagged proteins were used, and for RAB GTPases and R-SNARE proteins, wild-type plants expressing each of fluorescently tagged proteins were used for crossing. For labeling vacuolar membranes in plants expressing mGFP-VPS18 or VPS39-mGFP, Arabidopsis roots were incubated in liquid MS medium plus 4 μM FM4-64 for 3 h at RT. The 3D image was reconstructed using Image J (https://imagej.nih.gov/ij/) with the 3D project plug-in (https://imagej.net/Z-functions). The colocalization analysis between cytoplasmic punctate structures was performed as described previously (46). Pearson's colocalization coefficients were calculated using Image J with the PSC Colocalization plug-in (47).

For observation of embryos, seeds were cleared according to the method described previously (48) and observed with a fluorescence microscope (model BX51; Olympus) equipped with a confocal scanner unit (model CSU10; Yokogawa Electric) and a cooled CCD camera (model ORCA-AG; Hamamatsu Photonics).

For observing phenotypes of amiRNA lines, FM4-64 transport experiments and localization of pHGFP-VTI11 as well as YFP-VAMP711, live cell CLSM imaging was done using a Leica TCS SP5II microscope (Leica Microsystems) equipped with a Leica HCX PL APO lambda blue 63.0 × 1.20 UV water immersion objective operated by the Leica Application Suite Advanced Fluorescence software. For transmitted light imaging of root tips, 6–8-d-old heterozygous amiR-*vps3*, amiR-*vps8*, and amiR-*vps39* T2 seedlings grown on 1/2 MS medium supplemented with 30 μM DEX were observed. Fluorescence imaging of vacuole morphology was performed on 5-d-old heterozygous amiR-*vps3* and amiR-*vps39* T2 and homozygous amiR-*vps8* T3 seedlings transferred for 72 h to 1/2 MS medium containing 30 μM DEX. Vacuole lumen was stained with 10 μM BCECF, and 1 μM FM4-64 was used to label the plasma membrane (49). For FM4-64 pulse-chase experiments, the seedlings were grown on vertical 1/2 MS plates for 5 d and then transferred to vertical plates containing 1/2 MS medium supplemented with 30 μM DEX for 3 d. The staining pulse of 30 min was performed in liquid 1/2 MS medium containing 1 μM FM4-64, 30 μM DEX, and 1% perfluorodecalin solution (Sigma Aldrich). Subsequently, the seedlings were transferred to a washing solution of liquid 1/2 MS medium containing 30 μM DEX. Images were taken 20, 60, and 120 min after the start of the staining pulse. To observe the localization of pHGFP-VTI11 and YFP-VAMP711 on DEX induction, homozygous plants expressing the fluorescent fusion proteins were crossed with heterozygous amiR-*vps3* and amiR-*vps39* T2, as well as homozygous amiR-*vps8* T3 plants. Seedlings of the F2 progeny were grown similar to the seedlings for the FM4-64 experiments and selected according to their phenotypes. For the DMSO controls, the 1/2 MS plates contained similar amounts of DMSO instead of DEX. For quantification of YFP-VAMP711 signal intensity, the line profile quantification tool of the Leica Application Suite Advanced Fluorescence software was used. The fluorescence intensity of cytoplasmic punctae and the closest vacuolar membrane labeled by YFP-VAMP711 was determined and their ratio calculated. Statistical analysis was performed with OriginPro 2017 (OriginLabs). Image postprocessing operations were done with Fiji (Fiji Is Just ImageJ, based on ImageJ 1.51d; fiji.sc/Fiji; ref. 50).

**Yeast Two-Hybrid Assays.** For *VPS11*, *VPS3*, and *VPS39*, the ORF was subcloned into pBD-GAL4-GWRFC and pAD-GAL4-GWRFC provided from Demura and coworkers (51). Plasmids containing each *VPS* were introduced into the AH109 yeast strain (Clontech). Empty vectors were used for negative controls. Transformation was performed independently at least twice, and at least three colonies per transformation were checked for interaction.

**Antibodies.** For expression of GFP, the DNA fragment containing cDNA for GFP and the NOS terminator was subcloned into the pGEX 6P-1 vector (GE Healthcare) and introduced into *Escherichia coli* Rosetta (DE3) (Novagen). The construct for expressing GST-RABG3f was described previously (29), and purified proteins were used as antigens for immunizing rabbits. Anti-GFP antiserum was affinity-purified using the GST-GFP-coupled HiTrap NHS-activated HP Column (GE Healthcare), according to the manufacturer's instructions. We immunized two rabbits for GST-RABG3f, and obtained antisera were affinity-purified using HiTrap protein G HP Columns (GE Healthcare), according to the manufacturer's instructions. We examined the specificity of antibodies using lysates prepared from yeast cells expressing each of eight Arabidopsis RABG members. Both antisera reacted with RABG members except for RABG3b and RABG1, and we used one of the anti-RABG3f antibodies (#1) as the anti-RAB7 antibody in this study. Anti-ARA7 and anti-RHA1 antibodies were described in refs. 29 and 52, respectively. For detection of RAB5, we used a mixture of anti-ARA7 and anti-RHA1 antibodies at dilutions of 1:200 (anti-ARA7) and 1:100 (anti-RHA1). Anti-GFP and anti-RAB7 were used at 1:100, and anti-rabbit IgG was used at 1:5,000 (GE Healthcare).

**Immunoprecipitation and Mass Spectrometry.** For immunoprecipitation followed by mass spectrometry in Fig. 1 *B* and *C*, 6-d-old seedlings of transgenic plants expressing GFP or mGFP-VPS18 were soaked in crosslinking buffer [PBS (pH 7.4) and 1 mM dithiobis (succinimidyl propionate) (Thermo Fisher Scientific)] for 1 h at RT (room temperature). Tris·HCl (pH 7.5) was then added to 20 mM and incubated for 30 min at RT. Samples were ground in lysis buffer supplied in the micro-MACS GFP-tagged protein isolation kit (Miltenyi Biotec), and debris was then removed by centrifugation at 1,000 × *g* for 10 min at 4 °C. Supernatants were incubated for 60 min at 4 °C for solubilization, centrifuged at 20,000 × *g* for 10 min at 4 °C, and used for immunoprecipitation according to the manufacturer's instructions. Immunoprecipitates were separated by SDS/PAGE and stained using Flamingo Fluorescent Gel Stain (BIO-RAD). After lanes were cut from the gel, they were dehydrated with acetonitrile for 5 min and dried in a vacuum desiccator. The gel slices were then deoxidized in 10 mM DTT and 25 mM $NH_4HCO_3$ at 56 °C for 1 h, washed with 25 mM $NH_4HCO_3$ for 10 min, and alkylated with 55 mM iodoacetamide and 25 mM $NH_4HCO_3$ at RT for 45 min. Then, gel slices were washed with 25 mM $NH_4HCO_3$, dehydrated with 50% acetonitrile and 25 mM $NH_4HCO_3$ for 10 min twice, and dried. After incubating with 10 μg/mL trypsin in 50 mM $NH_4HCO_3$ on ice for 30 min, excess solution was removed, and the gel slices were incubated at 37 °C overnight. Digested peptides were extracted with 50% acetonitrile and 5% $CF_3COOH$ at RT for 30 min, and then extraction was repeated with new extraction solution. The peptides were dissolved in 30% acetonitrile and 0.1% formic acid, and then analyzed with Orbitrap Elite (Thermo Fisher Scientific), using Proteome Discoverer (Thermo Fisher Scientific).

For immunoprecipitation followed by Western blotting and mass spectrometry in Figs. 2 *A*–*C* and 7 *E* and *F*, respectively, 9-d-old transgenic seedlings expressing GFP, mGFP-VPS3, VPS39-mGFP, mGFP-VAMP713, or mGFP-VAMP727 were homogenized in grinding buffer [250 mM Sorbitol, 50 mM Hepes at pH 7.5, 2 mM EGTA, 0.5 mM $MgCl_2$, and one tablet of cOmplete EDTA-free (Roche)/50 mL]. Lysates were centrifuged at 1,000 × *g* for 10 min at 4 °C to remove debris. GTPγS (Sigma) and $MgCl_2$ were then added to the lysate to 0.1 mM and 1 mM, respectively, and incubated for 5 min at RT, followed by incubation for 1 h at 4 °C. After incubation for 5 min at RT, dithiobis (succinimidyl propionate) was added to 1 mM and incubated for 1 h at 4 °C. Tris·HCl (pH 7.5) and Triton X-100 were then added to 20 mM and 1%, respectively, and incubated for 1 h at 4 °C. Samples were centrifuged at 20,000 × *g* for 10 min at 4 °C to remove debris, and supernatants were used for immunoprecipitation using the micro-MACS GFP-tagged protein isolation kit (Miltenyi Biotec) according to the manufacturer's instructions, except for the column wash step; the columns were washed five times with wash buffer (grinding buffer + 1% Triton X-100, 1 mM $MgCl_2$ and 0.1 mM GTPγS).

**ACKNOWLEDGMENTS.** We thank Dr. M. T. Morita (Nagoya University, Japan), Dr. S. Mano (National Institute for Basic Biology, Japan), Dr. T. Demura (Nara Institute of Science and Technology, Japan), and Dr. T. Nakagawa (Shimane University, Japan) for sharing materials, as well as the Arabidopsis Biological Research Center and the Salk Institute for providing Arabidopsis mutants. Technical support was provided by the Functional Genomics Facility, NIBB Core Research Facilities, and the Model Plant Research Facility, NIBB BioResource Center. This work was financially supported by Grants-in-Aid for Scientific Research from the Ministry of Education, Culture, Sports, Science, and Technology of Japan (15K18551 to K.E.; 24114003, 15H04382, and 17K19412 to T.U.; and 25221103 to A.N.), Japan Science and Technology Agency, Precursory Research for Embryonic Science and Technology (JPMJPR11B2), a Grant-in-Aid for Japan Society for the Promotion of Science fellows (14J09222 to K.T.), The Mitsubishi Foundation, and Yamada Science Foundation.

1. Zhang C, Hicks GR, Raikhel NV (2014) Plant vacuole morphology and vacuolar trafficking. *Front Plant Sci* 5:476.
2. Ebine K, et al. (2014) Plant vacuolar trafficking occurs through distinctly regulated pathways. *Curr Biol* 24:1375–1382.
3. Viotti C, et al. (2010) Endocytic and secretory traffic in Arabidopsis merge in the trans-Golgi network/early endosome, an independent and highly dynamic organelle. *Plant Cell* 22:1344–1357.
4. Ueda T, Uemura T, Sato MH, Nakano A (2004) Functional differentiation of endosomes in Arabidopsis cells. *Plant J* 40:783–789.
5. Ebine K, et al. (2011) A membrane trafficking pathway regulated by the plant-specific RAB GTPase ARA6. *Nat Cell Biol* 13:853–859.
6. Ueda T, Yamaguchi M, Uchimiya H, Nakano A (2001) Ara6, a plant-unique novel type Rab GTPase, functions in the endocytic pathway of *Arabidopsis thaliana*. *EMBO J* 20:4730–4741.

7. Anuntalabhochai S, Terryn N, Van Montagu M, Inzé D (1991) Molecular characterization of an *Arabidopsis thaliana* cDNA encoding a small GTP-binding protein, Rha1. *Plant J* 1:167–174.
8. Wickner W, Schekman R (2008) Membrane fusion. *Nat Struct Mol Biol* 15:658–664.
9. Fujiwara M, et al. (2014) Interactomics of Qa-SNARE in *Arabidopsis thaliana*. *Plant Cell Physiol* 55:781–789.
10. Ebine K, et al. (2008) A SNARE complex unique to seed plants is required for protein storage vacuole biogenesis and seed development of *Arabidopsis thaliana*. *Plant Cell* 20:3006–3021.
11. Peplowska K, Markgraf DF, Ostrowicz CW, Bange G, Ungermann C (2007) The CORVET tethering complex interacts with the yeast Rab5 homolog Vps21 and is involved in endo-lysosomal biogenesis. *Dev Cell* 12:739–750.
12. Seals DF, Eitzen G, Margolis N, Wickner WT, Price A (2000) A Ypt/Rab effector complex containing the Sec1 homolog Vps33p is required for homotypic vacuole fusion. *Proc Natl Acad Sci USA* 97:9402–9407.
13. Nickerson DP, Brett CL, Merz AJ (2009) Vps-C complexes: Gatekeepers of endolysosomal traffic. *Curr Opin Cell Biol* 21:543–551.
14. Ostrowicz CW, et al. (2010) Defined subunit arrangement and rab interactions are required for functionality of the HOPS tethering complex. *Traffic* 11:1334–1346.
15. Cabrera M, et al. (2010) Phosphorylation of a membrane curvature-sensing motif switches function of the HOPS subunit Vps41 in membrane tethering. *J Cell Biol* 191: 845–859.
16. Balderhaar HJ, Ungermann C (2013) CORVET and HOPS tethering complexes - coordinators of endosome and lysosome fusion. *J Cell Sci* 126:1307–1316.
17. Cabrera M, et al. (2013) Functional separation of endosomal fusion factors and the class C core vacuole/endosome tethering (CORVET) complex in endosome biogenesis. *J Biol Chem* 288:5166–5175.
18. Huizing M, et al. (2001) Molecular cloning and characterization of human VPS18, VPS 11, VPS16, and VPS33. *Gene* 264:241–247.
19. Caplan S, Hartnell LM, Aguilar RC, Naslavsky N, Bonifacino JS (2001) Human Vam6p promotes lysosome clustering and fusion in vivo. *J Cell Biol* 154:109–122.
20. Pols MS, ten Brink C, Gosavi P, Oorschot V, Klumperman J (2013) The HOPS proteins hVps41 and hVps39 are required for homotypic and heterotypic late endosome fusion. *Traffic* 14:219–232.
21. Lachmann J, Glaubke E, Moore PS, Ungermann C (2014) The Vps39-like TRAP1 is an effector of Rab5 and likely the missing Vps3 subunit of human CORVET. *Cell Logist* 4: e970840.
22. Perini ED, Schaefer R, Stöter M, Kalaidzidis Y, Zerial M (2014) Mammalian CORVET is required for fusion and conversion of distinct early endosome subpopulations. *Traffic* 15:1366–1389.
23. Klinger CM, Klute MJ, Dacks JB (2013) Comparative genomic analysis of multi-subunit tethering complexes demonstrates an ancient pan-eukaryotic complement and sculpting in Apicomplexa. *PLoS One* 8:e76278.
24. Vukašinović N, Žárský V (2016) Tethering complexes in the Arabidopsis endomembrane system. *Front Cell Dev Biol* 4:46.
25. Rojo E, Gillmor CS, Kovaleva V, Somerville CR, Raikhel NV (2001) VACUOLELESS1 is an essential gene required for vacuole formation and morphogenesis in Arabidopsis. *Dev Cell* 1:303–310.
26. Tan X, Wei J, Li B, Wang M, Bao Y (2017) AtVps11 is essential for vacuole biogenesis in embryo and participates in pollen tube growth in Arabidopsis. *Biochem Biophys Res Commun* 491:794–799.
27. Hao L, Liu J, Zhong S, Gu H, Qu LJ (2016) AtVPS41-mediated endocytic pathway is essential for pollen tube-stigma interaction in Arabidopsis. *Proc Natl Acad Sci USA* 113:6307–6312.
28. Rojo E, Zouhar J, Kovaleva V, Hong S, Raikhel NV (2003) The AtC-VPS protein complex is localized to the tonoplast and the prevacuolar compartment in Arabidopsis. *Mol Biol Cell* 14:361–369.
29. Goh T, et al. (2007) VPS9a, the common activator for two distinct types of Rab5 GTPases, is essential for the development of *Arabidopsis thaliana*. *Plant Cell* 19: 3504–3515.
30. Sato MH, et al. (1997) The AtVAM3 encodes a syntaxin-related molecule implicated in the vacuolar assembly in *Arabidopsis thaliana*. *J Biol Chem* 272:24530–24535.
31. Nordmann M, et al. (2010) The Mon1-Ccz1 complex is the GEF of the late endosomal Rab7 homolog Ypt7. *Curr Biol* 20:1654–1659.
32. Leshem Y, Golani Y, Kaye Y, Levine A (2010) Reduced expression of the v-SNAREs AtVAMP71/AtVAMP7C gene family in Arabidopsis reduces drought tolerance by suppression of abscisic acid-dependent stomatal closure. *J Exp Bot* 61:2615–2622.
33. Cui Y, et al. (2014) Activation of the Rab7 GTPase by the MON1-CCZ1 complex is essential for PVC-to-vacuole trafficking and plant growth in Arabidopsis. *Plant Cell* 26: 2080–2097.
34. Singh MK, et al. (2014) Protein delivery to vacuole requires SAND protein-dependent Rab GTPase conversion for MVB-vacuole fusion. *Curr Biol* 24:1383–1389.
35. Hicks GR, Rojo E, Hong S, Carter DG, Raikhel NV (2004) Geminating pollen has tubular vacuoles, displays highly dynamic vacuole biogenesis, and requires VACUOLESS1 for proper function. *Plant Physiol* 134:1227–1239.
36. Niihama M, Takemoto N, Hashiguchi Y, Tasaka M, Morita MT (2009) ZIP genes encode proteins involved in membrane trafficking of the TGN-PVC/vacuoles. *Plant Cell Physiol* 50:2057–2068.
37. Mano S, Hayashi M, Nishimura M (1999) Light regulates alternative splicing of hydroxypyruvate reductase in pumpkin. *Plant J* 17:309–320.
38. Inada N, et al. (2016) Modulation of plant RAB GTPase-mediated membrane trafficking pathway at the interface between plants and obligate biotrophic pathogens. *Plant Cell Physiol* 57:1854–1864.
39. Segami S, Makino S, Miyake A, Asaoka M, Maeshima M (2014) Dynamics of vacuoles and H+-pyrophosphatase visualized by monomeric green fluorescent protein in Arabidopsis: Artifactual bulbs and native intravacuolar spherical structures. *Plant Cell* 26:3416–3434.
40. Geldner N, et al. (2009) Rapid, combinatorial analysis of membrane compartments in intact plants with a multicolor marker set. *Plant J* 59:169–178.
41. Lampropoulos A, et al. (2013) GreenGate—A novel, versatile, and efficient cloning system for plant transgenesis. *PLoS One* 8:e83043.
42. Karimi M, Inzé D, Depicker A (2002) GATEWAY vectors for Agrobacterium-mediated plant transformation. *Trends Plant Sci* 7:193–195.
43. Schwab R, Ossowski S, Riester M, Warthmann N, Weigel D (2006) Highly specific gene silencing by artificial microRNAs in Arabidopsis. *Plant Cell* 18:1121–1133.
44. Craft J, et al. (2005) New pOp/LhG4 vectors for stringent glucocorticoid-dependent transgene expression in Arabidopsis. *Plant J* 41:899–918.
45. Moore I, Samalova M, Kurup S (2006) Transactivated and chemically inducible gene expression in plants. *Plant J* 45:651–683.
46. Ito E, et al. (2012) Dynamic behavior of clathrin in *Arabidopsis thaliana* unveiled by live imaging. *Plant J* 69:204–216.
47. Krebs M, et al. (2010) Arabidopsis V-ATPase activity at the tonoplast is required for efficient nutrient storage but not for sodium accumulation. *Proc Natl Acad Sci USA* 107:3251–3256.
48. Aida M, Ishida T, Fukaki H, Fujisawa H, Tasaka M (1997) Genes involved in organ separation in Arabidopsis: An analysis of the cup-shaped cotyledon mutant. *Plant Cell* 9:841–857.
49. Viotti C, et al. (2013) The endoplasmic reticulum is the main membrane source for biogenesis of the lytic vacuole in Arabidopsis. *Plant Cell* 25:3434–3449.
50. Schindelin J, et al. (2012) Fiji: An open-source platform for biological-image analysis. *Nat Methods* 9:676–682.
51. Yamaguchi M, Kubo M, Fukuda H, Demura T (2008) Vascular-related NAC-DOMAIN7 is involved in the differentiation of all types of xylem vessels in Arabidopsis roots and shoots. *Plant J* 55:652–664.
52. Haas TJ, et al. (2007) The Arabidopsis AAA ATPase SKD1 is involved in multivesicular endosome function and interacts with its positive regulator LYST-INTERACTING PROTEIN5. *Plant Cell* 19:1295–1312.